Scientific Research Publishing

Journal of Geoscience and Environment Protection, 2022, 10, 145-166
https://www.scirp.org/journal/gep
ISSN Online: 2327-4344
ISSN Print: 2327-4336

Mineral Chemistry, Geobarometry and Oxygen Fugacity of the Granitic Rocks from the Itremo Domain, Central Madagascar

Désiré Alphonse Rakotondravaly[1,2*], Roger Randrianja[2]

[1]Directorate of Operations Monitoring, Ministry of Mines and Strategic Resources, Antananarivo, Madagascar
[2]Doctoral School of Engineering and Geosciences, University of Antananarivo, Antananarivo, Madagascar
Email: *drakotondravaly@yahoo.fr

How to cite this paper: Rakotondravaly, D. A., & Randrianja, R. (2022). Mineral Chemistry, Geobarometry and Oxygen Fugacity of the Granitic Rocks from the Itremo Domain, Central Madagascar. *Journal of Geoscience and Environment Protection, 10,* 145-166.
https://doi.org/10.4236/gep.2022.104010

Received: March 19, 2022
Accepted: April 18, 2022
Published: April 21, 2022

Copyright © 2022 by author(s) and Scientific Research Publishing Inc.
This work is licensed under the Creative Commons Attribution International License (CC BY 4.0).
http://creativecommons.org/licenses/by/4.0/

Open Access

Abstract

Major and accessory minerals from the Ibity granite, Tsarasaotra monzonitic and granite dykes, and Antsahakely granite of the Itremo domain in the Precambrian basement of Madagascar were characterized by using microscopic observations and chemical analyses with the aim of understanding their chemical characteristics and estimating the crystallization pressure and oxygen fugacity of their host rocks. Plagioclases in these rocks are albite and oligoclase, while alkali feldspars are orthoclase. For the phlogopite-micas, Fe-biotite and Li-phengite are common for the Ibity and Antsahakely granites, Mg-biotite is common for the Ibity granite and the Tsarasaotra monzonitic and granite dykes, and siderophyllite and Zinnwaldite are specific to the Ibity granite. Phlogopite-micas in the studied rocks are mainly primary, accessorily re-equilibrated, and rarely secondary. Calcic amphiboles distributed in the Magnesio-and Ferro-hornblende are identified in the Tsarasaotra monzonitic, whereas amphibole is rare and absent in the other rocks. Igneous titanite is observed in the Ibity granite and in the Tsarasaotra monzonitic rocks, which have similar compositions to some REE oxide-rich titanites. Concerning the Fe-Ti oxide phases, the rhombohedral and spinel/trifer tetroxide phases are found in both the Tsarasaotra monzonitic and the Tsarasaotra granite dyke, the trifer tetroxide and spinel + wüstite phases are found only in the Ibity granite, and the pseudobrookite + rhombohedral phase is found only in the Tsarasaotra granite dyke. The epidote mineral, rarely found in the Antsahakely granite, could be an indicator of metamorphism or hydrothermal activity involved during the emplacement of this rock. Aluminum in hornblende geobarometer gave pressure ranges of around 5 kbar for the Tsarasaotra monzonitic rocks. The Titanite geobarometer gave pressures of 2.5 - 3.2 kbar for the Ibity granite, 2.9 kbar for the Tsarasaotra monzonitic, and 7.1 kbar for the

Antsahakely granite. Both amphibole and Fe-Ti oxide-base oxygen fugacity reveal high oxygen fugacity conditions for the Tsarasaotra monzonitic and granite dyke emplacements, which might have a relationship with a porphyritic environment.

Keywords

Itremo, Granitic, Monzonitic, Mineral Chemistry, Geobarometer, Fugacity

1. Introduction

Among the geodynamic domains of the Precambrian terrane of Madagascar, the Itremo domain is located in the center-south of Madagascar, surrounding the Ambatofinandrahana district and Ibity town, which are two famous places in terms of mineral potential and productivity in Madagascar (Lacroix, 1922). These mineral potentials, composed of gemstones and semi-precious stones as industrial ores, have been operated by small-scale mining operators as well as by companies for decades (e.g. Ravoniarisoa & Rakotomanana, 2002).

Several works discuss the petrology and the geochemistry of the magmatic suites in the Itremo domain, such as the Imorona-Itsindro suite (Handke, Tucker, & Ashwal, 1999; McMillan et al., 2003; Moine, Bosse, Paquette, & Ortéga, 2014; Rasoamalala et al., 2014; Tucker, Roig, Moine, Delor, & Peters, 2014; Yang et al., 2015) and the Ambalavao suite (Roig, Tucker, Peters, Delor, & Theveniaut, 2012; Tucker, Peters, Roig, Théveniaut, & Delor, 2012; Tucker, Roig, Moine, Delor, & Peters, 2014; Rasoamalala et al., 2014). Other studies are related to the metamorphic rocks in the Itremo domain (Cox, Armstrong, & Ashwal, 1998; Morteani & Ackermand, 2006; Tucker, Kusky, Buchwaldt, & Handke, 2007). The majority of magmatism-related works were based on whole rock geochemistry approaches, with a primary emphasis on the petrology and geochemistry of these magmatic rocks as isotopic and geochronological studies. A mineral chemistry-based approach such as Rasoamalala et al. (2014) was lacking for the study of these rocks, as well as the geographic distribution and relationships among the two magmatic suites in the Itremo domain. Moine, Nédélec, & Ortéga (2014) build on previous work on the geology of Madagascar's Precambrian terrane, particularly in terms of geological cartography. Recent work by Rakotondravaly & Randrianja (2022) contributes to these works by providing more information related to the geographical distribution of these two magmatic suites in the Itremo domain, as well as the membership and possible relationships of the granitic rocks in that domain. However, mineral chemistry information regarding these rocks remains poorly documented.

This work aims at studying the mineral chemistry of the granitic rocks in the Itremo domain, and will focus on the study of the main minerals from the Tsarasaotra monzonitic and granite dyke, the Ibity and the Ambatofinandrahana granites from the Itremo domain, as well as their formation environment by us-

ing geochemical approaches. Mineral chemistry studies of these rocks will provide additional information regarding their geochemical characteristics.

2. Geological Setting of the Study Area

The Itremo domain is among the nine (09) divisions of the tectonometamorphic domains of the Madagascar Precambrian socle (Collins & Windley, 2002; Moine, Nédélec, & Ortéga, 2014), which is mainly composed of Archean rocks in the North and Proterozoic rocks in the South (Yoshida, 1998; Roig, Tucker, Peters, Delor, & Theveniaut, 2012; Tucker, Roig, Moine, Delor, & Peters, 2014). This domain consists of parametamorphic formations composed of schist, quartzite, and cipolin known as the Schisto-Quartzo-Dolomite formation or Itremo group, which is intruded by the Imorona-Itsindro suite and the Ambalavao suite (Roig, Tucker, Peters, Delor, & Theveniaut, 2012) (**Figure 1**).

The Imorona-Itsindro suite, composed of gabbro and diorite, and granite typical of calc-alkaline porphyritic massive granite (Moine, 1974; Daso, 1986; Tucker,

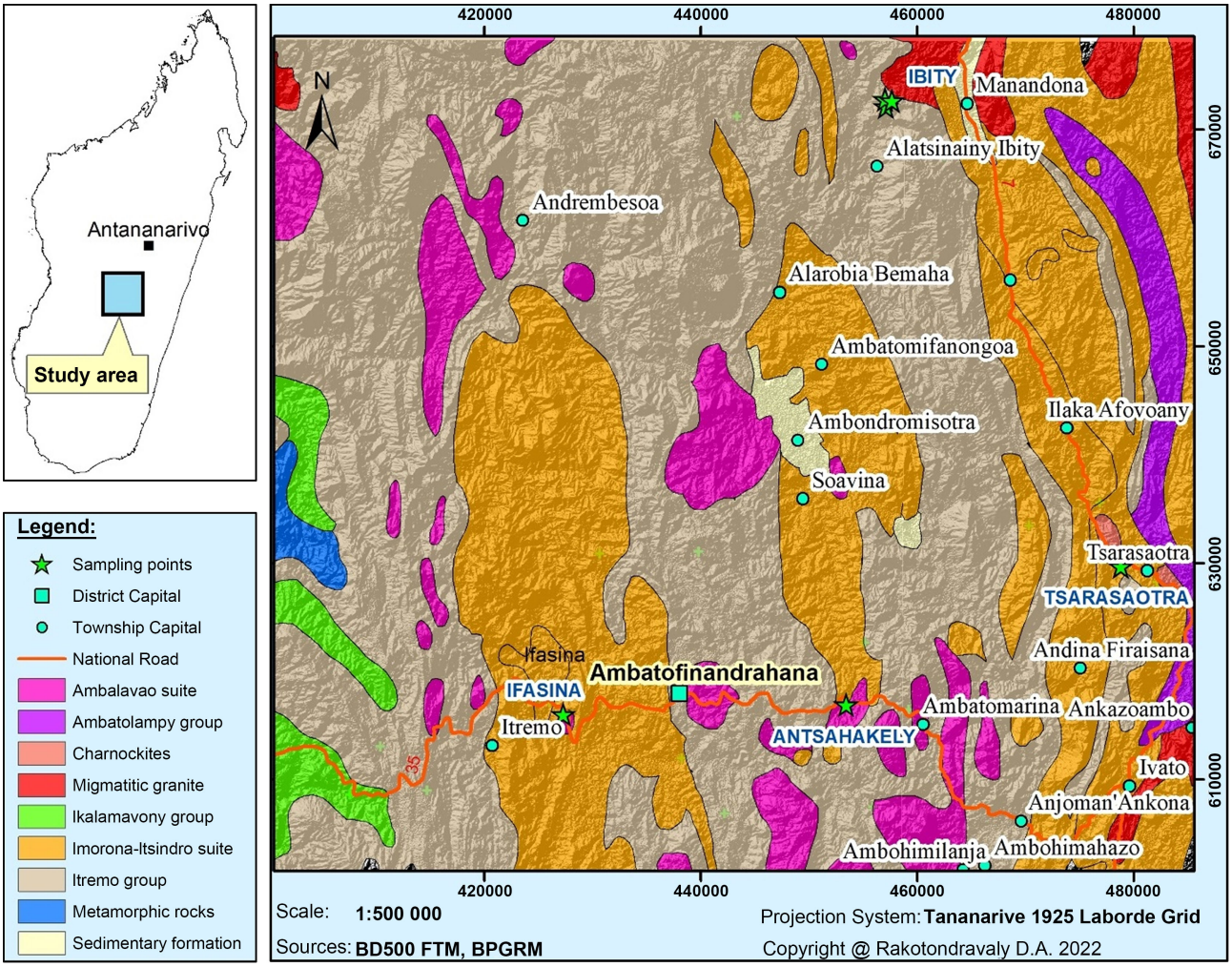

Figure 1. (Top left)—map of Madagascar showing the study area; (right)—simplified geologic map of the Itremo domain after Roig et al. (2012); Rasoamalala et al. (2014) and Archibald et al. (2016) with sampling points of this study.

Peters, Roig, Théveniaut, & Delor, 2012), is thought to have been emplaced by: 1) crustal extension before 747 Ma, followed by 2) lithospheric subduction and arc magmatism around and after 729 - 727 Ma (Yang et al., 2015). The Ambalavao suite, composed of alkali-potassic plutonic formations (essentially granite and syenite) (Emberger, 1956; Tucker, Peters, Roig, Théveniaut, & Delor, 2012), is thought to have been emplaced by the magmatic events related to the continental collision between East and West Gondwana between 580 and 520 Ma (Tucker et al., 1999; Archibald et al., 2019).

3. Sampling and Analytical Techniques

Field research was carried out in the Itremo domain in the outcrops of Ibity (around 20.049˚S and 46.983˚E), Tsarasaotra Ambositra (20˚26'15.7"S and 47˚11'35.1"E), and Antsahakely (20˚33'14.8"S and 46˚57'01.6"E). A dozen granitic rock samples were collected for laboratory investigations at the Faculty of International Resource Sciences of Akita University, Japan.

Microscopic observations of slide glass-covered thin sections were performed by using a NIKON ECLIPSE 50i microscope. Polished thin sections and polished samples were made for both microscopic observation and qualitative and quantitative microanalysis under JEOL SUPERPROBE JXA-733. Quantitative analyses of silicates and oxides were conducted with an accelerating voltage of 15 KeV, an electron beam of 20 nA, and 5 to 10 μm in diameter. The measuring time for the standard is 10 s repeated 5 times, and that of the background is 40 s. A Lithium Fluoride (LiF) crystal was used to detect Fe Kα and Mn Kα, Pentaerythritol (PET) crystal for K Kα, Ti Kα, Ca Kα and Thallium Acid Phthalate (TAP) crystal for Na Kα, Si Kα, Mg Kα and Al Kα. As standards, SiO_2, TiO_2, Al_2O_3, Fe_2O_3, MnO, MgO, $CaSiO_3$, $NaAlSi_3O_8$, and $KAlSi_3O_8$ minerals were used. Bence & Albee (1968)'s procedures were used to correct the data.

4. Petrography

More detailed petrographic descriptions can be found in Rakotondravaly & Randrianja (2022).

The Ibity granitic rocks are mainly leucocratic holocrystalline pseudo-idiomorphic grainy granite classified as granite, after Le Maitre et al. (2002) classification scheme. It is essentially composed of plagioclase, alkali feldspar, and quartz, and its accessorily minerals are mafic silicate minerals, magnetite, ilmenite, apatite, and zircon in trace (**Figure 2**).

The Tsarasaotra principal granitic rocks are mesocratic holocrystalline hypidiomorphic medium-to-coarse grained rocks which are classified into monzonite and quartz monzonite after Le Maitre et al. (2002) classification scheme. They are mainly composed of plagioclase, alkali feldspar, and mafic silicate minerals, and their accessory minerals are quartz, magnetite, ilmenite, apatite, and zircon (**Figure 2**).

The Tsarasaotra granitic dykes are leucocratic holocrystalline pseudo-idiomorphic coarse-grained rocks classified as granite after Le Maitre et al. (2002)

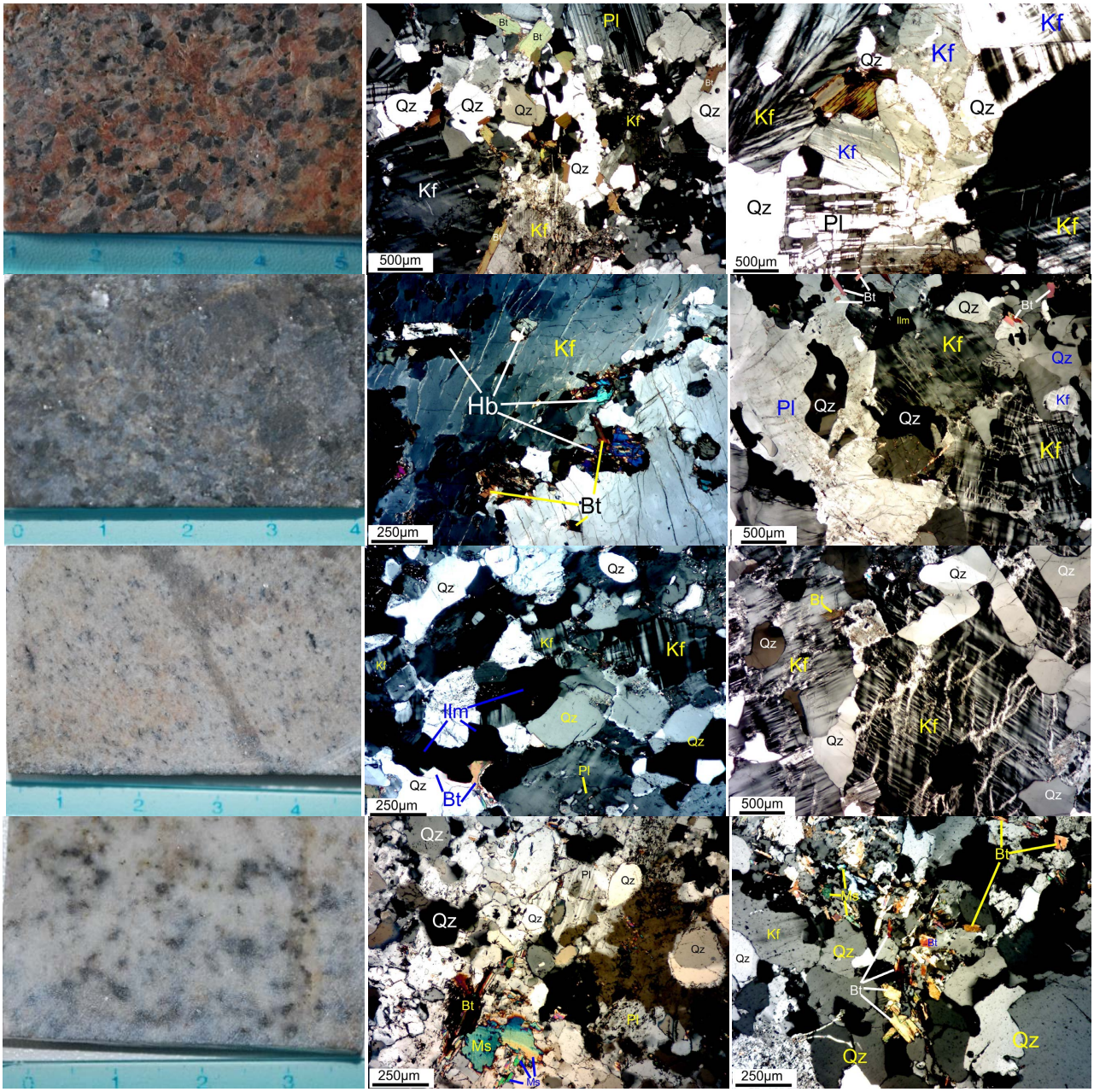

Figure 2. Representative photographs (left) and microphotographs (center and right) of the studied rocks. From top to bottom: Ibity granite, Tsarasaora monzonitic rocks, Tsarasaotra granite dykes, and Antsahakely granite.

classification scheme. They are essentially made of plagioclase, alkali feldspar, and quartz, and their accessory minerals are mafic silicate minerals, magnetite, ilmenite, apatite, and zircon in trace (**Figure 2**).

The Ambatofinandrahana granitic rocks are leucocratic holocrystalline hypidiomorphic medium-to-coarse grained rocks which are classified into granite after Le Maitre et al. (2002) classification scheme. These rocks are essentially composed of plagioclase, alkali feldspar, and quartz, and their accessory minerals are mafic silicate minerals, magnetite, ilmenite, apatite, and zircon in trace (**Figure 2**).

5. Mineral Chemistry

5.1. Feldspars

The structural formulae of plagioclase feldspars were recalculated on the basis of 8 oxygens. Representative electron microprobe data of plagioclase is shown in Table 1.

For the Ibity granite, plagioclases are albite (An 1.38 - 7.50) and oligoclase (An 10.50 - 24.09). Albites have SiO_2 concentrations of 64.07 - 69.57 wt%, Al_2O_3 concentrations of 21.28 - 23.06 wt%, CaO concentrations of 0.24 - 1.52 wt%, and Na_2O concentrations of 8.72 - 10.73 wt%. Oligoclases have concentrations of SiO_2 = 62.16 - 67.35 wt%, Al_2O_3 = 21.66 - 25.38 wt%, CaO = 2.04 - 3.07 wt% and Na_2O = 5.19 - 10.49 wt%. Alkali feldspars are orthoclase (Or 92.19 - 97.71) having concentrations in SiO_2 = 60.11 - 66.02 wt%, Al_2O_3 = 18.22 - 20.55 wt%, Na_2O = 0.27 - 0.88 wt%, and K_2O = 15.69 - 18.33 wt% (Table 1 and Figure 3).

Table 1. Representative electron microprobe analyses of plagioclase and alkali feldspars from the studied rocks.

Rocks	Ibity				Tsarasaotra				Ibity		Tsarasaotra				Antsahakely	
	Granite				Monzonitic		Granite dyke		Granite		Monzonitic		Granite dyke		Granite	
Spl	IB-8	IB-8	IB-8	IB-16	TS-6	TS-6	TS-2	TS-2	IB-9A	IB-14	TS-1	TS-6	TS-2	TS-4	ANH-1	ANH-1
Point	PL-3	PL-1C	PL-3	PL-1A	PL-2	PL-2A	PL-1	PL-2	KF-3	KF-1	KF-3	KF-1	KF-1	KF-2	KF-4	KF-5
SiO_2	64.1	67.3	64.7	69.1	68.3	65.7	65.0	63.9	65.9	62.6	64.4	63.6	45.6	64.4	64.6	61.3
TiO_2		0.01		-	0.01	0.00		0.02	0.00	0.02	0.03	0.03	0.10		-	0.01
Al_2O_3	23.1	25.4	23.3	22.2	21.9	23.3	22.8	24.1	18.5	19.3	19.9	19.3	35.3	19.7	19.0	19.9
FeO	0.05	0.04	0.02	0.03	0.09	0.08	0.01	0.07	-	0.03	0.04	0.03	3.33	0.02	-	0.04
MnO		-		-	-	-		0.00	-		0.01	-			-	
MgO		-	0.00	-	0.02	-	0.00	-	-	0.00	0.01	-	0.43		-	
CaO	1.52	3.02	2.04	0.24	0.73	1.86	2.58	4.28	0.01	-	0.59	0.04		0.04	0.01	
Na_2O	10.25	5.19	9.48	9.58	10.3	9.95	9.70	8.62	0.88	0.28	1.61	0.58	0.17	1.26	0.48	0.34
K_2O	0.19	0.11	0.17	0.07	0.02	0.13	0.13	0.35	15.9	18.3	14.5	16.5	11.4	16.1	17.1	17.5
Total	99.1	101	100	101	101	101	100	101	101	101	101	100	96.3	102	101	99.0
Si	2.84	2.87	2.84	2.95	2.93	2.85	2.85	2.78	3.00	2.92	2.93	2.95	2.22	2.94	2.97	2.90
Ti	-	0.00	-	-	0.00	0.00	-	0.00	0.00	0.00	0.00	0.00	0.00	-	-	0.00
Al	1.20	1.27	1.21	1.12	1.11	1.19	1.18	1.24	1.00	1.06	1.07	1.05	2.02	1.06	1.03	1.11
Fe	0.00	0.00	0.00	0.00	0.00	0.00	0.00	0.00	-	0.00	0.00	0.00	0.14	0.00	-	0.00
Mn	-	-	-	-	-	-	-	0.00	-	-	0.00	-	-	-	-	-
Mg	-	-	0.00	-	0.00	-	0.00	-	-	0.00	0.00	-	0.03	-	-	-
Ca	0.07	0.14	0.10	0.01	0.03	0.09	0.12	0.20	0.00	-	0.03	0.00	-	0.00	0.00	-
Na	0.88	0.43	0.81	0.79	0.86	0.84	0.82	0.73	0.08	0.03	0.14	0.05	0.02	0.11	0.04	0.03
K	0.01	0.01	0.01	0.00	0.00	0.01	0.01	0.02	0.92	1.09	0.84	0.97	0.71	0.94	1.00	1.05
An	7.50	24.1	10.5	1.38	3.8	9.3	12.7	21.1	0.04	-	2.8	0.2	-	0.2	0.04	-
Ab	91.4	74.8	88.4	98.2	96.1	89.9	86.5	76.9	7.77	2.29	14.0	5.1	2.2	10.6	4.10	2.85
Or	1.09	1.07	1.06	0.45	0.14	0.80	0.73	2.03	92.2	97.7	83.2	94.8	97.8	89.2	95.9	97.2

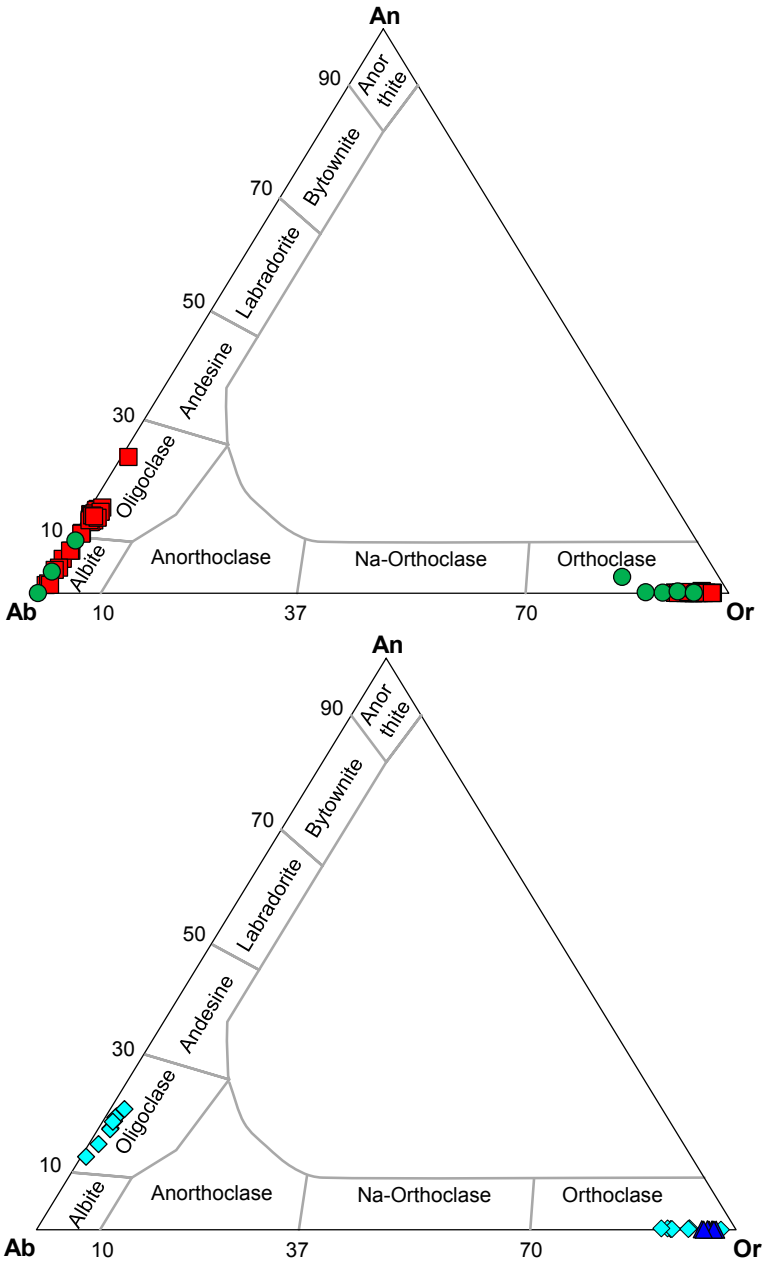

Figure 3. Classification diagrams for feldspars from the studied rocks. Red square: Ibity granite, green circle: Tsarasaotra monzonitic; magenta diamond: Tsarasaotra granite dykes; and blue triangle: Antsahakely granite.

Regarding the Tsarasaotra monzonitic rocks, plagioclases are distributed in albite (An 3.78 - 9.29) with concentrations of SiO_2 = 65.72 - 68.32 wt%, Al_2O_3 = 21.89 - 23.29 wt%, CaO = 0.73 - 1.86 wt%, and Na_2O = 9.95 - 10.32 wt%. Alkali feldspars are orthoclase (Or 83.16 - 94.93), with SiO_2 concentrations of 62.08 - 64.44 wt%, Al_2O_3 concentrations of 18.92 - 20.21 wt%, Na_2O concentrations of 0.58 - 1.61 wt%, and K_2O concentrations of 14.53 - 16.96 wt% (Table 1 and Figure 3).

Plagioclases are distributed in oligoclases (An 12.73 - 21.09) in the Tsarasaotra

granitic dykes, with SiO_2 = 62.16 - 65.34 wt%, Al_2O_3 = 22.85 - 24.75 wt%, CaO = 2.58 - 4.28 wt%, and Na_2O = 8.58 - 9.70 wt%. Alkali feldspars are orthoclase (Or 89.22 - 97.83) with SiO_2 concentrations of 45.63 - 64.39 wt%, Al_2O_3 concentrations of 18.92 - 35.26 wt%, Na_2O concentrations of 0.17 - 1.26 wt%, and K_2O concentrations of 11.39 - 17.83 wt% (**Table 1** and **Figure 3**).

For the Antsahakely granite, plagioclases are rare, so analyses were focused on alkali feldspars. Alkali feldspars are orthoclase (Or 95.06 - 97.15), having compositions of SiO_2 = 61.26 - 64.91 wt%, Al_2O_3 = 19.01 - 20.15 wt%, Na_2O = 0.34 - 0.58 wt%, and K_2O = 17.13 - 17.50 wt% (**Table 1** and **Figure 3**).

5.2. Phlogopite-Micas

On the basis of 11 oxygens, the structural formulae of plagioclase feldspars were recalculated. Representative electron microprobe data of plagioclase and their calculated formulae are given in Lithium composition estimates and the classification diagram are after Tischendorf et al. (1997). Then, the 10 × TiO_2-MgO-FeO^T + MnO ternary system was proposed by (Nachit, Ibhi, Abia, & Ohoud, 2005) for discriminating primary, re-equilibrated primary, and secondary biotite.

For the Ibity granite, phlogopite-micas are distributed mainly within the siderophyllite, Fe-biotite, and Mg-biotite zones, accessorily within the Li-phengite zone, and rarely in the Zinnwaldite zone (**Figure 4**). Siderophyllites in the Ibity granite have concentrations of SiO_2 = 35.71 - 37.98 wt%, TiO_2 = 1.13 - 2.80 wt%, Al_2O_3 = 16.62 - 17.43 wt%, FeO = 19.83 - 29.28 wt%, MgO = 3.62 - 5.71 wt%, K_2O = 9.42 - 10.59 wt%, and Li_2O = 0.66 - 1.32 wt%. Fe-biotites have compositions of SiO_2 = 34.20 - 38.36 wt%, TiO_2 = 0.56 - 3.80 wt%, Al_2O_3 = 14.87 - 20.62 wt%, FeO = 14.01 - 26.78 wt%, MgO = 3.75 - 7.83 wt%, K_2O = 9.36 - 13.18 wt%, and Li_2O = 0.23 - 0.84 wt%. Then, Mg-biotites have concentrations of SiO_2 = 34.45 - 38.07 wt%, TiO_2 = 2.28 - 3.31 wt%, Al_2O_3 = 15.06 - 16.90 wt%, FeO = 17.58 - 20.88 wt%, MgO = 10.15 - 11.63 wt%, K_2O = 6.06 - 10.37 wt%, and Li_2O = 0.08 - 0.12 wt%. Regarding Li-phengites, they have compositions of SiO_2 = 41.74 - 45.08 wt%, TiO_2 = 0.03 - 0.78 wt%, Al_2O_3 = 30.82 - 34.54 wt%, FeO = 4.56 - 5.06 wt%, MgO = 0.20 - 2.20 wt%, K_2O = 10.59 - 11.20 wt%, and Li_2O = 2.41 - 3.37 wt%. Concerning the Zinnwaldites, they have concentrations of SiO_2 = 45.39 wt%, TiO_2 = 0.27 wt%, Al_2O_3 = 32.71 wt%, FeO = 6.35 wt%, MgO = 1.08 wt%, K_2O = 10.49 wt%, and Li_2O = 3.46 wt%. Biotite in the Ibity granite is distributed mainly in the domain of primary and re-equilibrated primary biotite and rarely in the secondary biotite (**Table 2** and **Figure 5**).

For the Tsarasaotra monzonitic rocks and Tsarasaotra granitic dykes, phlogopite-micas are Mg-biotites. For the monzonitic rocks, they have compositions of SiO_2 = 36.67 - 37.51 wt%, TiO_2 = 2.74 - 4.01 wt%, Al_2O_3 = 14.18 - 15.18 wt%, FeO = 16.15 - 19.73 wt%, MgO = 10.38 - 12.46 wt%, K_2O = 9.98 - 10.60 wt%, and Li_2O = 0.06 - 0.11 wt%, while the granitic dykes have concentrations of SiO_2 = 34.93 - 37.24 wt%, TiO_2 = 2.25 - 3.11 wt%, Al_2O_3 = 14.60 - 15.15 wt%, FeO = 18.01 - 18.70 wt%, MgO = 10.39 - 11.27 wt%, K_2O = 10.27 - 11.08 wt%, and Li_2O

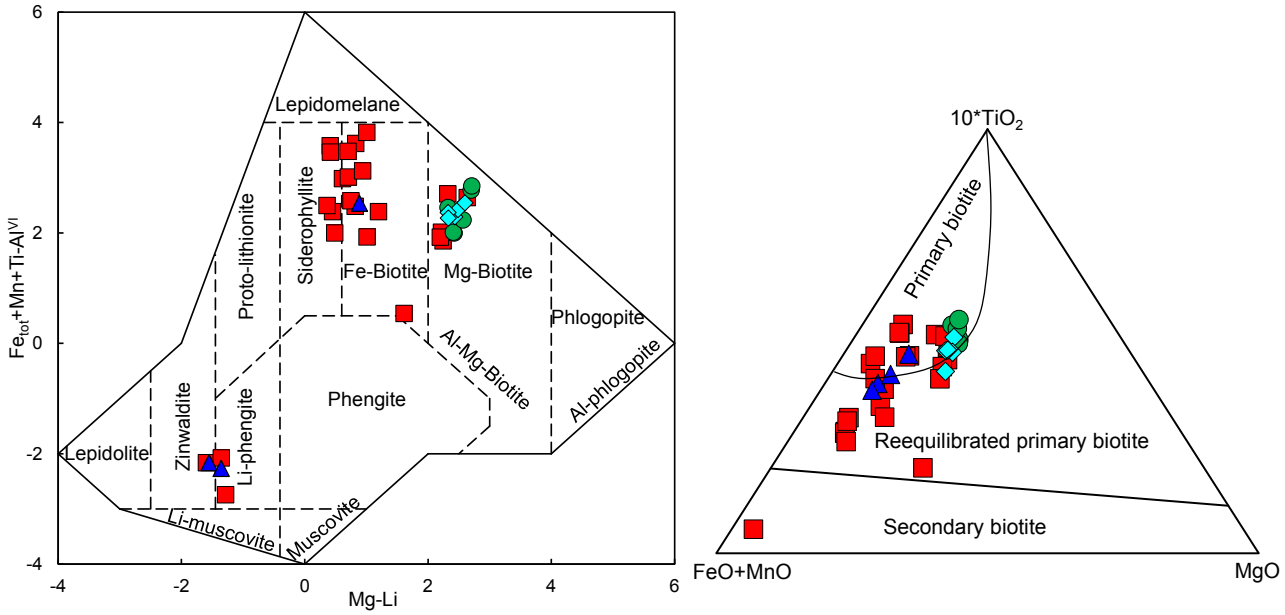

(a) (b)

Figure 4. (a) Classification diagram of phlogopite-mica after Tischendorf et al. (1997); (b) discrimination of biotite after Nachit, Ibhi, Abia, & Ohoud (2005) (right). Legend follows **Figure 3**.

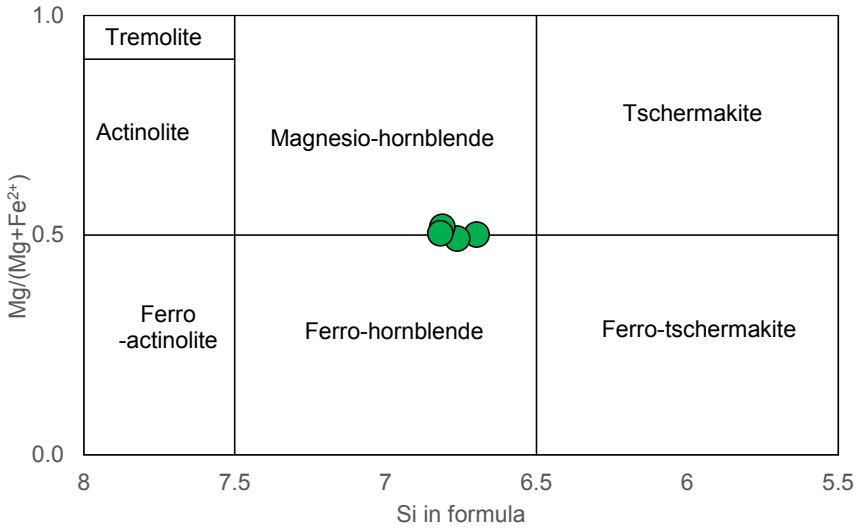

Figure 5. Classification diagram of amphibole for the Tsarasaotra monzonitic after Leake et al. (1997).

= 0.08 - 0.11 wt%. Except a rare re-equilibration signature identified for the granite dyke sample TS-2 (10 × TiO_2 = 22.46 wt%; FeO + MnO = 19.03 wt%; MgO = 10.89 wt%), all other biotites are primary (**Table 2** and **Figure 5**).

For the Ambatofinandrahana granites, phlogopite-micas are distributed in the Fe-biotite, Zinnwaldite, and Li-phengite fields (Figure). SiO_2 = 34.77 wt%, TiO_2 = 1.98 wt%, Al_2O_3 = 18.76 wt%, FeO = 24.31 wt%, MgO = 4.83 wt%, K_2O = 7.69 wt%, and Li_2O = 0.39 wt% are the compositions of Fe-biotite in these rocks. Zinnwaldite has compositions of SiO_2 = 45.69 wt%, TiO_2 = 0.53 wt%, Al_2O_3 =

Table 2. Representative electron microprobe analyses of phlogopite-micas from the studied rocks.

Rock sample	Ibity						Tsarasaotra			Antsahakely
	Granite						Monzonite	Granite dykes		Granite
	IB-6	IB-6	IB-8	IB-14	IB-16A	IB-16A	TS-6	TS-3	TS-3	ANH-1
wt%	BI-1	BI-2	BI-1	BI-1	BI-1	BI-3	BI-2	BI-1	BI-2	BI-1
SiO_2	38.4	38.0	35.7	34.2	34.5	38.1	37.5	37.2	34.9	34.8
TiO_2	2.28	2.26	1.13	2.16	2.32	2.68	2.89	3.11	2.69	1.98
Al_2O_3	16.9	17.3	17.4	17.0	16.9	16.7	14.9	14.9	14.6	18.8
FeO	19.5	19.8	23.7	25.6	20.9	17.8	17.4	18.3	18.2	24.3
MnO	0.62	0.59	0.53	0.71	0.65	0.40	0.43	0.44	0.43	0.45
MgO	6.03	5.71	3.68	4.56	11.6	10.2	11.6	11.2	11.3	4.83
CaO	-	0.05	0.04	0.01	0.26	0.01	0.03	0.03	0.01	0.30
Na_2O	0.05	0.08	0.04	0.07	0.07	0.09	0.06	0.05	0.04	0.03
K_2O	10.7	10.6	10.0	10.6	6.06	9.91	10.6	10.4	11.1	7.7
Li_2O	0.59	1.32	0.66	0.23	0.08	0.12	0.08	0.09	0.08	0.39
Total	95.0	95.7	93.0	95.2	93.3	95.9	95.5	95.8	93.3	93.5
Number of cations recalculated on the basis of 11 oxygens.										
Si	5.87	5.76	5.71	5.46	5.34	5.71	5.69	5.65	5.51	5.48
Al^{IV}	2.13	2.24	2.29	2.54	2.66	2.29	2.31	2.35	2.49	2.52
Al^{VI}	0.91	0.85	1.00	0.66	0.42	0.66	0.37	0.32	0.23	0.96
Ti	0.26	0.26	0.14	0.26	0.27	0.30	0.33	0.36	0.32	0.23
Fe	2.49	2.51	3.18	3.42	2.71	2.23	2.21	2.33	2.40	3.20
Mn	0.08	0.08	0.07	0.10	0.09	0.05	0.06	0.06	0.06	0.06
Mg	1.38	1.29	0.88	1.09	2.69	2.27	2.62	2.54	2.65	1.13
Ca	-	0.01	0.01	0.00	0.04	0.00	0.00	0.00	0.00	0.05
Na	0.01	0.02	0.01	0.02	0.02	0.02	0.02	0.01	0.01	0.01
K	2.08	2.05	2.04	2.17	1.20	1.90	2.05	2.02	2.23	1.55
Li	0.36	0.80	0.43	0.14	0.05	0.07	0.05	0.05	0.05	0.25
XMg	0.36	0.34	0.22	0.24	0.50	0.50	0.54	0.52	0.53	0.26
XNa	0.01	0.01	0.01	0.01	0.02	0.01	0.01	0.01	0.01	0.01
Mg-Li	1.01	0.49	0.45	0.94	2.64	2.20	2.57	2.49	2.60	0.89
Fe + Mn + Ti-Al^{VI}	1.93	2.00	2.38	3.12	2.64	1.92	2.23	2.42	2.55	2.54

33.50 wt%, FeO = 5.81 wt%, MgO = 1.39 wt%, K_2O = 11.19 wt%, and Li_2O = 3.54 wt%, whereas Li-phengite has compositions of SiO_2 = 43.72 wt%, TiO_2 = 0.44 wt%, Al_2O_3 = 33.90 wt%, FeO = 5.94 wt%, MgO = 1.09 wt%, K_2O = 11.12 wt%, and Li_2O = 2.98 wt%. Except for a primary biotite observed (10 × TiO_2 = 6.01 wt%; FeO + MnO = 5.25 wt%; MgO = 1.54 wt%), other biotites were objects of re-equilibration (Table 2 and Figure 5).

5.3. Amphiboles

Structural formulae of amphiboles were recalculated on the basis of 23 oxygen (22 oxygen and 2OH) by following the procedures after Li et al. (2020). Representative chemical compositions of amphibole determined by electron microprobe analyses and their calculated formulae are given in Table. Nomenclature and classification diagram is after Leake et al. (1997).

In the studied rocks, amphiboles were identified and analyzed in the Tsarasaotra monzonitic rocks. They are calcic amphiboles with $Ca_B \geq 1.50$ and $(Na + K)_A < 0.50$. These amphiboles distribute in the Magnesio and Ferro-hornblende (Si = 6.70 - 6.82; Mg# = 0.49 - 0.52; $(Na + K)_A = 0.34 - 0.40$ et $Ca_A = 0.00$) according to the classification diagram (Figure). They have concentrations of SiO_2 = 42.34 - 44.86 wt%, TiO_2 = 0.86 - 1.37 wt%, FeO = 15.96 - 16.78 wt%, MgO = 7.93 - 8.84 wt%, CaO = 10.69 - 11.50 wt%, Na_2O = 1.56 - 1.66 wt%, and K_2O = 1.30 - 1.46 wt% (**Table 3** and **Figure 5**).

Table 3. Representative microprobe analyses of amphiboles from the studied rocks.

	Tsarasaotra			
	TS-1	TS-1	TS-1	TS-1
wt%	PX-1	PX-2	AM-1	AM-2
SiO_2	42.3	44.2	44.8	44.9
TiO_2	1.31	1.37	0.86	0.92
Al_2O_3	9.04	9.13	9.06	9.05
FeO*	16.0	16.8	16.3	16.6
MnO	0.57	0.50	0.56	0.53
MgO	7.93	8.32	8.84	8.62
CaO	10.7	11.4	11.4	11.5
Na_2O	1.58	1.66	1.56	1.61
K_2O	1.43	1.46	1.36	1.30
Total	90.8	94.8	94.7	95.0
Number of cations recalculated on the basis of 23 oxygens.				
Si	6.70	6.76	6.81	6.82
Al^{IV}	1.32	1.23	1.18	1.17
Ti	-	0.01	0.01	0.01
Sum T	8.01	8.00	8.00	8.00
Al^{VI}	0.37	0.42	0.44	0.45
Ti	0.17	0.14	0.09	0.10
Fe^{3+}	0.43	0.35	0.39	0.36
Mn	0.06	0.06	0.06	0.06
Mg	1.87	1.90	2.01	1.95
Fe^{2+}	1.86	1.96	1.86	1.92

Continued

Sum C	4.77	4.84	4.85	4.85
Mn	0.01	0.01	0.01	0.01
Fe^{2+}	-	-	-	-
Mg	-	-	-	-
Ca	1.82	1.88	1.86	1.88
Na	0.43	0.38	0.38	0.38
Sum B	2.26	2.26	2.24	2.26
Ca	-	-	-	-
Na	0.05	0.12	0.08	0.10
K	0.29	0.28	0.26	0.25
Sum A	0.34	0.40	0.35	0.35
Mg#	0.50	0.49	0.52	0.50
(Na + K)A	0.34	0.40	0.35	0.35

5.4. Titanite

The structural formulae of titanites were recalculated on the basis of five oxygens. Representative microprobe analyses of titanites with recalculated formulae are shown in **Table 4**.

Among the studied rocks, the Ibity granite, the Tsarasaotra monzonitic rocks, and the Antsahakely granite all contain some titanite minerals.

For the Ibity granite, titanites have compositions of SiO_2 = 29.91 - 30.42 wt%, TiO_2 = 28.95 - 34.84 wt%, Al_2O_3 = 1.87 - 2.56 wt%, FeO = 1.90 - 2.17 wt%, MnO = 0.11 - 0.28 wt%, and CaO = 25.96 - 26.72 wt% (**Table 4**), which are similar to those of the black titanite in the Quoscescer pegmatite in the North-East of Harar, Ethiopia. That black titanite also contains P_2O_5 (0.06 wt%), BaO (0.04 wt%), ZrO_2 (in trace) as well as REE oxides such as Ce_2O_3 (2.98 wt%) and Y_2O_3 (1.53 wt%) (Deer, Howie, & Zussman, 2013).

Titanite in the Tsarasaotra monzonitic rocks has concentrations of SiO_2 = 29.68 wt%, TiO_2 = 34.86 wt%, Al_2O_3 = 2.32 wt%, FeO = 2.21 wt%, MnO = 0.29 wt%, and CaO = 25.61 wt% (**Table 4**).

Regarding the Antsahakely granite, the observed titanite has the compositions of SiO_2 = 29.16 wt%, TiO_2 = 30.11 wt%, Al_2O_3 = 6.40 wt%, FeO = 3.16 wt%, MnO = 0.13 wt%, and CaO = 25.51 wt% (**Table 4**).

Based on Aleinikoff et al. (2002)'s diagram, titanites in the Ibity granite and Tsarasaotra monzonitic rocks are magmatism-related (Al = 0.08 - 1.00; Fe = 0.05 - 0.06) and (Al = 0.09; Fe = 0.06), respectively, whereas those of the Antsahakely granite have a metamorphic origin (Al = 0.26; Fe = 0.09) (**Figure 6**).

5.5. Fe-Ti Oxides

The structural formulae were recalculated on the basis of four oxygens for the magnetite and three oxygens for the ilmenite, as well as Fe^{2+} and Fe^{3+} components

Table 4. Representative microprobe analyses of titanite from the studied rocks.

wt%	Ibity				Tsarasaotra	Antsahakely.
	IB-16A/ KUR-1	IB-16A/ KUR-2	IB-16A/ BI-4	IB-16A/ SPH-1	TS-6/MT-2	ANH-1/BI-3
SiO_2	30.4	30.4	30.1	29.9	29.7	29.2
TiO_2	28.9	30.8	34.6	34.8	34.9	30.1
Al_2O_3	1.87	2.11	2.56	2.34	2.32	6.40
FeO	2.06	2.11	2.17	1.90	2.21	3.16
MnO	0.26	0.28	0.19	0.11	0.29	0.13
MgO	0.02	0.02	0.08	0.06	0.06	0.43
CaO	26.3	26.0	26.6	26.7	25.6	25.5
Total	89.8	91.6	96.2	95.9	95.0	94.9
Si	1.10	1.08	1.02	1.02	1.02	1.00
Ti	0.79	0.82	0.88	0.89	0.90	0.78
Al	0.08	0.09	0.10	0.09	0.09	0.26
Fe^{2+}	0.06	0.06	0.06	0.05	0.06	0.09
Mn	0.01	0.01	0.01	0.00	0.01	0.00
Mg	0.00	0.00	0.00	0.00	0.00	0.02
Ca	1.02	0.99	0.97	0.98	0.94	0.94
Na	0.00	0.00	0.00	0.00	0.00	0.00
K	0.00	0.00	0.00	0.00	0.00	0.01

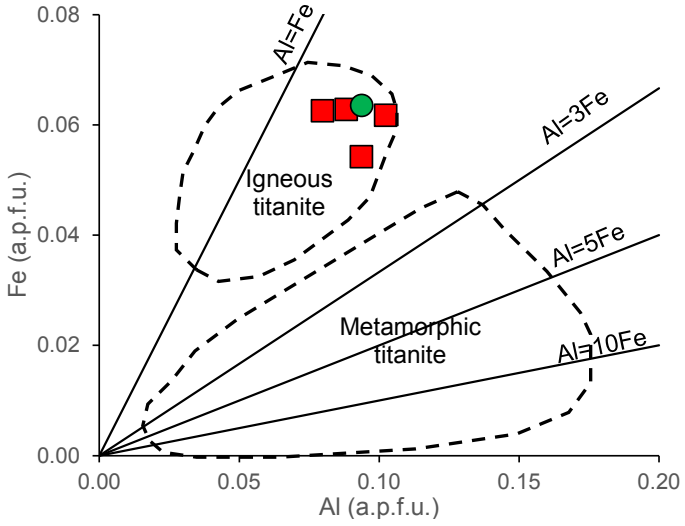

Figure 6. Classification diagram of titanite for the studied rocks. Legend follows **Figure 3**.

according to Carmichael (1966)'s method. The molar fractions in percent of Ulvöspinel (Usp mol%) and Ilmenite (Ilm mol%) were recalculated according to Carmichael (1966) and Lindsley & Spencer (1982)'s methods. In the studied rocks, Fe-Ti oxides were identified except in the Ambatofinandrahana granites, for which representative microprobe data are shown in **Table 5**.

Table 5. Representative electron microprobe analyses of magnetite and ilmenite from the studied rocks.

wt%	Ibity granite				Tsarasaotra monzonitic.	Trasaraotra granite		Tsarasaotra monzonitic		Tsarasaotra granite	
	IB-7A MT-1	IB-15 MT-1	IB-16A MT-1	IB-16A MT-2	TS-6 MT-1	TS-2 MT-1	TS-3 MT-3	TS-1 ILM-1	TS-1 ILM-3	TS-2 ILM-2	TS-3 ILM-2
SiO_2	0.04	0.01	0.04	0.03	0.04	0.10	0.05	0.01	0.03	0.07	0.04
TiO_2	0.05	0.04	0.01	0.02	0.02	0.00	0.04	42.7	46.5	9.4	46.0
Al_2O_3	0.07	0.06	0.04	0.02	0.08	0.04	0.10	0.01	0.01	0.02	0.01
FeO*	98.6	95.0	97.7	97.4	94.0	89.9	92.1	48.2	50.0	76.5	43.1
MnO	0.11	0.01	0.02	0.01	0.09		0.08	2.29	2.38	0.06	7.78
MgO	0.00	0.01	0.01		0.01		0.00	0.23	0.31	0.01	0.22
Total	98.8	95.1	97.8	97.4	94.2	90.0	92.4	93.4	99.2	86.1	97.2
Ferrous and ferric components recalculated after Carmichael (1966).											
SiO_2	0.04	0.01	0.04	0.03	0.04	0.10	0.05	0.01	0.03	0.07	0.04
TiO_2	0.04	0.04	0.01	0.02	0.02	0.00	0.04	42.7	46.5	9.4	46.0
Al_2O_3	0.06	0.06	0.04	0.02	0.08	0.04	0.10	0.01	0.01	0.02	0.01
Fe_2O_3	68.0	68.7	68.5	68.3	69.6	66.4	68.1	13.9	12.3	75.7	11.0
FeO	30.7	31.0	30.9	30.8	31.4	30.1	30.8	35.7	38.9	8.5	33.2
MnO	0.10	0.01	0.02	0.01	0.09	-	0.08	2.29	2.38	0.06	7.78
MgO	0.00	0.01	0.01	-	0.01	-	0.00	0.23	0.31	0.01	0.22
Total	99.0	99.8	99.5	99.2	101	96.7	99.2	94.8	100	93.7	98.3
Si	0.00	0.00	0.00	0.00	0.00	0.00	0.00	0.00	0.00	0.00	0.00
Ti	0.00	0.00	0.00	0.00	0.00	0.00	0.00	0.86	0.88	0.20	0.89
Al	0.00	0.00	0.00	0.00	0.00	0.00	0.00	0.00	0.00	0.00	0.00
Fe^{3+}	1.99	1.99	2.00	2.00	1.99	1.99	1.99	0.28	0.23	1.60	0.21
Fe^{2+}	1.00	1.00	1.00	1.00	1.00	1.00	1.00	0.80	0.82	0.20	0.72
Mn	0.00	0.00	0.00	0.00	0.00	-	0.00	0.05	0.05	0.00	0.17
Mg	0.00	0.00	0.00	-	0.00	-	0.00	0.01	0.01	0.00	0.01
Total	3.00	3.00	3.00	3.00	3.00	3.00	3.00	2.00	2.00	2.00	2.00
Usp/Ilm (%)	0.28%	0.16%	0.16%	0.00	0.22%	0.42%	0.33%	0.86	0.88	0.20	0.89

According to Taylor (1964) phase equilibria in the ternary system FeO-TiO_2-Fe_2O_3 at 1300˚C, the stable phases of Fe-Ti oxides in the Ibity granite are spinel under the Trifer tetroxide (TiO_2 = 0.01 wt%; FeO = 35.5 wt%; Fe_2O_3 = 38.4 wt%) and Spinel + wüstite (TiO_2 = 0.01 - 0.04 wt%; FeO = 30.7 - 31.0 wt%; Fe_2O_3 = 68.0 - 68.7 wt%) (**Table 5** and **Figure 7**).

For the Tsarasaotra monzonitic rocks, identified stable phases are spinel/trifer tetroxide (TiO_2 = 0.02 - 0.04 wt%; FeO = 31.4 - 32.3 wt%; Fe_2O_3 = 69.6 - 71.2 wt%) and rhombohedral (TiO_2 = 42.7 - 46.5 wt%; FeO = 35.7 - 38.9 wt%; Fe_2O_3 = 12.3 - 14.4 wt%) (**Table 5** and **Figure 7**).

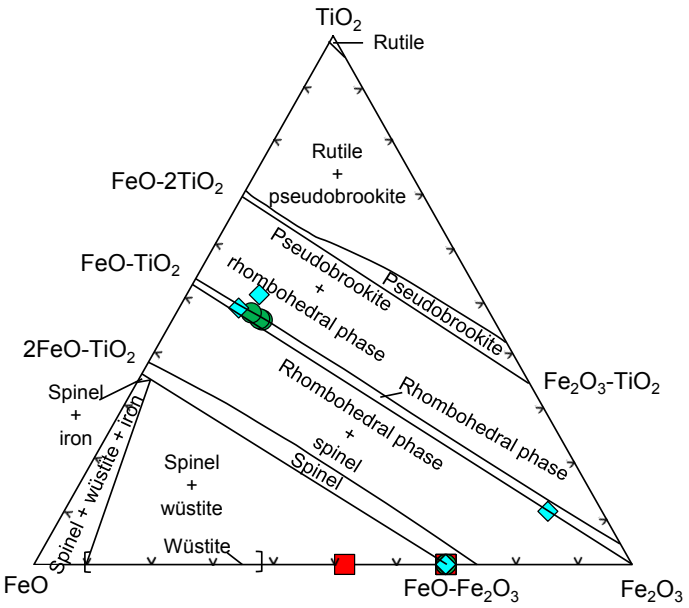

Figure 7. Phase equilibria diagram in the FeO-TiO_2-Fe_2O_3 ternary system at 1300˚C of the studied rocks after Taylor (1964). Legends follows **Figure 3**.

Concerning the Tsarasaotra granitic dykes, the spinel/trifer tetroxide phase (TiO_2 = 0.00 - 0.04 wt%; FeO = 30.1 - 31.6 wt%; Fe_2O_3 = 66.4 - 69.9 wt%) and pseudobrookite + rhombohedral phase (TiO_2 = 46.0 wt%; FeO = 33.2 wt%; Fe_2O_3 = 11.0 wt%) were observed in addition to the rhombohedral phase (TiO_2 = 9.40 wt%; FeO = 8.46 wt%; Fe_2O_3 = 75.7 wt% and TiO_2 = 47.4 wt%; FeO = 40.5 wt%; Fe_2O_3 = 9.76 wt%) (**Table 5** and **Figure 7**).

5.6. Epidote

The structural formula of epidote was recalculated on the basis of 12 oxygen atoms. Absent in most of the studied rocks and rare in the Antsahakely granite, epidote has concentrations of SiO_2 = 37.72 wt%, TiO_2 = 0.10 wt% Al_2O_3 = 25.14 wt%, FeO = 11.33 wt%, MnO = 0.61 wt%, and CaO = 22.42 wt% which is aluminum rich compared to that reported by Anthony (1990) of Westfield, Hampden County, Massachusetts, USA. The presence of epidote could be an indicator of a certain degree of metamorphism or hydrothermal activity in the Antsahakely granite.

6. Geobarometry and Oxygen Fugacity Estimates

6.1. Aluminum in Hornblende Geobarometer

The aluminum in hornblende geobarometry was applied to the Tsarasaotra monzonitic rocks in which amphiboles were identified and analyzed. The method proposed by Schmidt (1992) gives pressure estimates in the range of 4.7 to 5 kbars (±0.6 kbars) based on total aluminum in formula (Al^{tot} = 1.62 - 1.69), whereas Anderson & Smith (1995) provides pressures around 5 kbars (Fe/(Fe + Mg) = 0.53 - 0.55) (**Figure 8**).

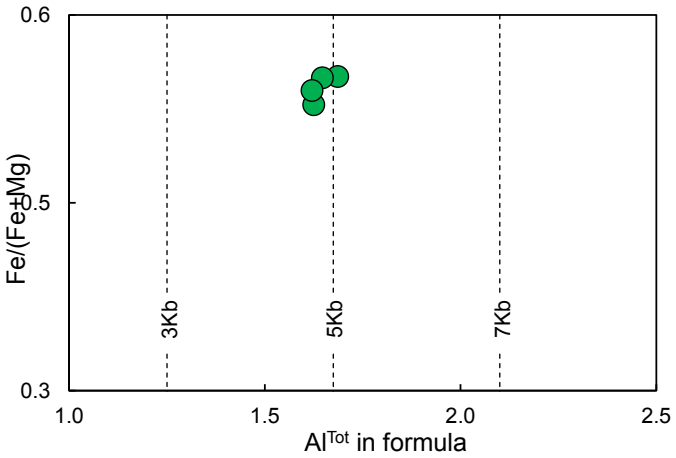

Figure 8. Estimated pressures based on Fe/(Fe + Mg) versus Al^{tot} in formula in amphiboles after Anderson & Smith (1995).

6.2. Titanite Geobarometer

Since titanite minerals were identified and analyzed in the Ibity granite, the Tsarasaotra monzonitic rocks, and the Antsahakely granite, the titanite geobarometer was applied to these rocks by using the method recently proposed by Erdmann et al. (2019). Based on Al_2O_3 content in weight percent, average pressures of 2.5 - 3.2 kbars, 2.9 kbars, and 7.1 kbars were obtained for the Ibity granite, the Tsarasaotra monzonitic, and the Antsahakely granite, respectively (**Table 6**).

6.3. Oxygen Fugacity

On the basis of Amphibole

An oxygen fugacity estimate was applied to the Tsarasaotra monzonitic rocks by using the method proposed by Anderson & Smith (1995). According to the Fe/(Fe + Mg) ratio versus the Al^{IV} expressed in atom per formula unit (apfu), regardless of the Al^{IV} content (0.37 - 0.45), the Tsarasaotra monzonitic rocks have Fe/(Fe + Mg) ratio less than 0.6 (0.53 - 0.55), indicating a formation condition with high oxygen fugacity (**Figure 9(a)**).

On the basis of Fe-Ti oxides

Oxygen fugacity and temperatures were also estimated by using the method proposed by Spencer & Lindsley (1981) according to the magnetite-ilmenite mineral assemblage. Based on this method, the Tsarasaotra rocks give oxygen fugacity estimates ranging from −18.2 to −17.5 for the monzonitic rocks and from −19.9 to −17.7 for the granite dyke. These results are above the NNO buffer, which indicates a formation under a highly oxidized environment. For comparison, the Tsarasaotra monzonitic rocks were formed under a similar oxidation environment as that of granitic rocks around the Kamaishi Cu-Fe skarn deposit as reported in Rakotondravaly (2018). The Tsarasaotra monzonitic rocks and granite dykes were both formed under much higher oxygen fugacity relative to the Yerington batholith (Dilles, 1987), which might indicate a porphyritic environment affinity (**Figure 9(b)**; **Table 7**).

Table 6. Results of Titanite geobarometer.

	Ibity				Tsarasaotra.	Antsahakely.
	Granite				Monzonitic	Granite
	IB-16A	IB-16A	IB-16A	IB-16A	TS-6	ANH-1
Oxide	KUR-1	KUR-2	BI-4	SPH-1	MT-2	BI-3
SiO_2	30.4	30.4	30.1	29.9	29.7	29.2
TiO_2	28.9	30.8	34.6	34.8	34.9	30.1
Al_2O_3	1.87	2.11	2.56	2.34	2.32	6.40
FeO	2.06	2.11	2.17	1.90	2.21	3.16
MnO	0.26	0.28	0.19	0.11	0.29	0.13
MgO	0.02	0.02	0.08	0.06	0.06	0.43
CaO	26.3	26.0	26.6	26.7	25.6	25.5
Total	89.8	91.6	96.2	95.9	95.0	94.9
Titanite geobarometer						
P (Kbar)	2.5	2.7	3.2	3.0	2.9	7.1

Table 7. Results of Temperature and oxygen fugacity estimates based on Fe-Ti oxide compositions.

	Tsarasaotra							
	Monzonitic				Granitic dyke			
	TS-6	TS-1	TS-6	TS-1	TS-2	TS-2	TS-3	TS-3
	MT-1	ILM-2	MT-2	ILM-3	MT-1	ILM-1	MT-3	MT-2
Data with recalculated ferrous and ferric components after Carmichael (1966).								
SiO_2	0.04	0.01	0.04	0.03	0.05	0.03	0.05	0.04
TiO_2	0.02	46.0	0.02	46.5	0.01	47.4	0.04	46.0
Al_2O_3	0.08	0.02	0.08	0.01	0.07	0.02	0.10	0.01
Fe_2O_3	69.6	14.4	69.6	12.3	69.2	9.8	68.1	11.0
FeO	31.4	38.6	31.4	38.9	31.3	40.5	30.8	33.2
MnO	0.09	2.30	0.09	2.38	0.02	1.86	0.08	7.78
MgO	0.01	0.26	0.01	0.31	0.00	0.16	0.00	0.22
CaO	0.01	0.01	0.01	0.01	0.00	0.00	0.00	0.01
Total	101	102	101	100	101	100	99.2	98.3
XUsp/XIlm	0.00	0.86	0.00	0.88	0.00	0.90	0.00	0.88
Fe-Ti geothermometer and oxygen fugacity after Spencer & Lindsley (1981).								
T (˚C)	482		474		437		504	
$\log_{10} f_{O2}$	−17.5		−18.2		−19.9		−17.7	
T (˚C) Average	478				471			

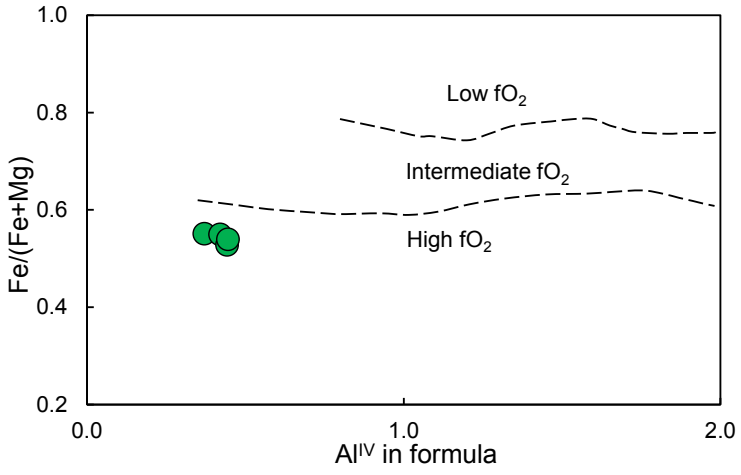

(a)

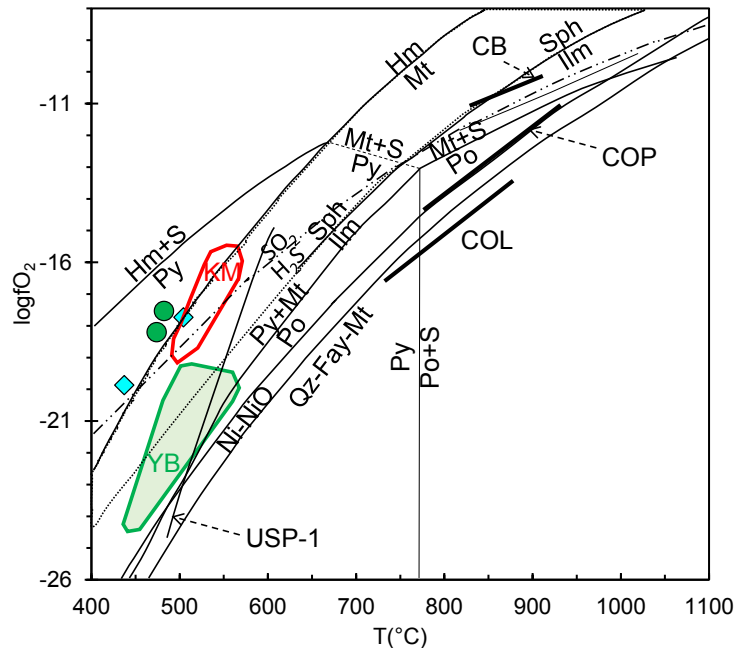

(b)

Figure 9. (a) Oxygen fugacity estimate based on Fe/(Fe + Mg) versus AlIV in formula in amphiboles (Anderson & Smith, 1995); and (b) oxygen fugacity versus temperature based on Fe-Ti oxides after Spencer & Lindsley (1981). HM-MT: hematite-magnetite (Chou, 1978); NNO: Ni-NiO (Huebner & Sato, 1970); and FMQ: quartz-fayalite-magnetite (Hewitt, 1978). COL, COP and CB are olivine ± clinopyroxene, othropyroxene ± clinopyroxene, and biotite + hornblende-bearing volcanic suites, respectively (Carmichael, 1966). YB: Yerington Batholith (Dilles, 1987); and KM: Kamaishi mine (Rakotondravaly, 2018). Legend follows **Figure 3**.

7. Conclusion

Plagioclase and alkali feldspars are among the main minerals found in the Ibity granite, the Tsarasaotra monzonitic and granite dykes, and the Antsahakely granite, while biotite, amphiboles, Fe-Ti oxide minerals, and titanite are accessory minerals.

Regarding the studied rocks, plagioclases are mainly distributed in albite and oligoclase, while alkali feldspars have a composition of orthoclase. Phlogopite-mica is distributed mostly in and around the biotite fields, and accessorily in and around the muscovite fields. Biotite is mostly distributed in the primary and re-equilibrated primary biotite fields. Amphibole is hornblende for the Tsarasaotra monzonitic, which is rare and absent for other studied rocks. Igneous titanite is observed in the Ibity granite and Tsarasaotra monzonitic, while titanite is not identified in the other studied rocks. The Fe-Ti oxide minerals of the studied rocks are found in both titanium-rich and titanium-free phases. An indication of either metamorphism or hydrothermal activity was observed in the Antsahakely granite.

The aluminum in hornblende geobarometer gave pressure estimates higher than the titanite geobarometer for the Tsarasaotra monzonitic rock. The Antsahakely granite most likely formed at a lower depth relative to the Ibity granite and the Tsarasaotra monzonitic, which formed at a similar depth.

The high oxygen fugacity estimated in the Tsarasaotra rocks could indicate an affinity for a porphyritic environment.

This work enlightens us regarding the main and accessory minerals in the granitic rocks from the studied area as well as the potential affinity of these rocks for a mineralization process. Additional investigations should be carried out, especially fluid inclusion studies, in order to better understand the possible fluid-mineral interaction relating to the emplacement of these rocks.

Acknowledgements

This research work was financially supported by the Japan International Cooperation Agency (JICA) as part of the human resource development capacity program for the mineral sector in developing countries. We gratefully thank Professor Daizo Ishiyama of the Faculty of International Resource Sciences, Akita University, Japan, for his advice on using EPMA equipment. We are also grateful to anonymous reviewers for their comments and suggestions, which contributed to the improvement of the final version of the manuscript.

Conflicts of Interest

The authors declare no conflicts of interest regarding the publication of this paper.

References

Aleinikoff, J. N., Wintsch, R. P., Fanning, C. M., & Dorais, M. J. (2002). U–Pb Geochronology of Zircon and Polygenetic Titanite from the Glastonbury Complex, Connecticut, USA: An integrated SEM, EMPA, TIMS, and SHRIMP Study. *Chemical Geology, 188,* 125-147. https://doi.org/10.1016/S0009-2541(02)00076-1

Anderson, J. L., & Smith, D. R. (1995). The Effects of Temperature and fO2 on the Al-in Hornblende Barometer. *American Mineralogist, 80,* 549-559. https://doi.org/10.2138/am-1995-5-614

Anthony, J. W. (1990). *Handbook of Mineralogy*. Mineral Data Publishing.

Archibald, D. B., Collins, A. S., Foden, J. D., Payne, J. L., Holden, P., & Razakamanana, T. (2019). Late Syn-to Post-Collisional Magmatism in Madagascar: The Genesis of the Ambalavao and Maevarano Suites. *Geoscience Frontiers, 10,* 2063-2084. https://doi.org/10.1016/j.gsf.2018.07.007

Archibald, D. B., Collins, A. S., Foden, J. D., Payne, J. L., Holden, P., Razakamanana, T. et al. (2016). Genesis of the Tonian Imorona-Itsindro Magmatic Suite in Central Madagascar: Insight from U-Pb, Oxygen and Hafnium Isotopes in Zircon. *Precambrian Research, 281,* 312-337. https://doi.org/10.1016/j.precamres.2016.05.014

Bence, A. E., & Albee, A. L. (1968). Empirical Correction Factors for the Electron Microanalysis of Silicates and Oxides. *Journal of Geology, 76,* 382-403. https://doi.org/10.1086/627339

Carmichael, I. S. (1966). The Iron-Titanium Oxides of Salic Volcanic Rocks and Their Associated Ferromagnesian Silicates. *Contributions to Mineralogy and Petrology, 14,* 36-64. https://doi.org/10.1007/BF00370985

Chou, I. M. (1978). Calibration of Oxygen Buffers at Elevated P and T Using Hydrogen Fugacity Sensor. *American Mineralogists, 63,* 690-703.

Collins, A. S., & Windley, B. F. (2002). The Tectonic Evolution of Central and Northern Madagascar and Its Place in the Final Assembly of Gondwana. *The Journal of Geology, 110,* 325-339. https://doi.org/10.1086/339535

Cox, R., Armstrong, R. A., & Ashwal, L. D. (1998). Sedimentology, Geochronology and Provenance of the Proterozoic Itremo Group, Central Madagascar, and Implications for Pre-Gondwana Palaeogeography. *Journal of the Geological Society, 155,* 1009-1024. https://doi.org/10.1144/gsjgs.155.6.1009

Daso, A. H. (1986). *Géologie d'une plateforme carbonatée métamorphique. Vallée de la Sahatany centre de Madagascar. Etude structurale, pétrographique et géochimique.* Université Paul Sabatier.

Deer, W. A., Howie, R. A., & Zussman, J. (2013). *An Introduction to the Rock-Forming Minerals* (3rd ed.). Longman Scientific & Technical. https://doi.org/10.1180/DHZ

Dilles, J. E. (1987). Petrology of the Yeringron Batolith, Nevada: Evidence for Evolution of Porphyry Copper Ore Fluids. *Economic Geology, 82,* 1750-1789. https://doi.org/10.2113/gsecongeo.82.7.1750

Emberger. (1956). *Notice explicative sur la feuille Itremo-Ambatofinandrahana.* Service Géologique de Tananarive.

Erdmann, S., Wang, R., Huang, F., Scaillet, B., Zhao, K., Liu, H. et al. (2019). Titanite: A Potential Solidus Barometer for Granitic Magma Systems. *Comptes Rendus Geoscience*, *351*, 551-561. https://doi.org/10.1016/j.crte.2019.09.002

Handke, M. J., Tucker, R. D., & Ashwal, L. D. (1999). Neoproterozoic Continental Arc Magmatism in West-Central Madagascar. *Geology, 27,* 351-354. https://doi.org/10.1130/0091-7613(1999)027%3C0351:NCAMIW%3E2.3.CO;2

Hewitt, D. A. (1978). A Redetermination of the Fayalite-Magnetite-Quartz Equilibrium between 650˚ and 850˚ C. *American Journal of Science, 278,* 715-724. https://doi.org/10.2475/ajs.278.5.715

Huebner, J. S., & Sato, M. (1970). The Oxygen Fugacity-Temperature Relationships of Manganese Oxide and Nickel-Nickel Oxide Buffers. *American Mineralogists, 55,* 934-952.

Lacroix, A. (1922). *Minéralogie de Madagascar Tome II: Minéralogie Appliquée-Lithologie* (éd. 1ère). Librairie Maritime et Coloniale.

Le Maitre, R., Streckeisen, A., Zanettin, B., Le Bas, M., Bonin, B., Bateman, P. et al (2002).

Igneous Rocks: A Classification and Glossary of Terms: Recommendations of the International Union of Geological Sciences Subcommission of the Systematics of Igneous Rocks (éd. 2nd). (L. Maitre, Éd.) Cambridge University Press. https://doi.org/10.1017/CBO9780511535581

Leake, B. E., Woolley, A. R., Arps, C. E., Brich, W. D., Charles Gilbert, M., Grice, J. D. et al. (1997). Nomenclature of Amphiboles: Report of the Subcommittee on Amphiboles of the International Mineralogical Association, Commission on New Minerals and Mineral Names. *The Canadian Mineralogist, 35,* 219-246.

Li, X., Zhang, C., Behrens, H., & Holtz, F. (2020). Calculating Amphibole Formula from Electron Microprobe Analysis Data Using a machine Learning Method Based on Principal Components Regression. *Lithos, 362-363,* Article ID: 105469. https://doi.org/10.1017/CBO9780511535581

Lindsley, D. H., & Spencer, K. J. (1982). Fe-Ti Oxide Geothermometry: Reducing Analyses of Coexisting Ti-Magnetite (Mt) and Ilmenite (ilm). *EOS Transactions American Geophysical Union, 63,* 471.

McMillan, A., Harris, N. W., Holness, M., Ashwal, L., Kelley, S., & Rambeloson, R. (2003). A Granite-Gabbro Complex from Madagascar: Constraints on Melting of the Lower Crust. *Contributions to Mineralogy and Petrology, 145,* 585-599. https://doi.org/10.1007/s00410-003-0470-1

Moine, B. (1974). *Caractères de sédimentation et métamorphisme des séries précambriennes épizonales à catazonales du centre de Madagascar (Région d'Ambatofinandrahana).* Université de Nancy I.

Moine, B., Bosse, V., Paquette, J.-L., & Ortéga, E. (2014). The Occurrence of a Tonian–Cryogenian (~850 Ma) Regional Metamorphic Event in Central Madagascar and the Geodynamic Setting of the Imorona–Itsindro (~800 Ma) Magmatic Suite. *Journal of African Earth Sciences, 94,* 58-73. https://doi.org/10.1016/j.jafrearsci.2013.11.016

Moine, B., Nédélec, A., & Ortéga, E. (2014). Geology and Metallogeny of the Precambrian Basement of Madagascar. *Journal of African Earth Sciences, 94,* 1-8. https://doi.org/10.1016/j.jafrearsci.2014.01.016

Morteani, G., & Ackermand, D. (2006). Mineralogy, Geochemistry and Petrology of an Amphibolite-Facies Aluminum-Phosphate and Borosilicate (APB)-Bearing Quartzite from the Mesoproterozoic Itremo Group (Central Madagascar). *Neues Jahrbuch für Mineralogie-Abhandlungen, 182,* 123-148. https://doi.org/10.1127/0077-7757/2006/0036

Nachit, H., Ibhi, A., Abia, E. H., & Ohoud, M. B. (2005). Discrimination between Primary Magmatic Biotites, Reequilibrated Biotites and Neoformed Biotites. *Comptes Rendus Geoscience, 337,* 1415-1420. https://doi.org/10.1016/j.crte.2005.09.002

Rakotondravaly, D. A. (2018). *Petrology and Geochemistry of the Intermediate Igneous Rocks from the Kamaishi Cu-Fe Skarn Deposit, Iwate Prefecture, Japan.* Unpublished Master's Thesis, Faculty of International Resource Sciences, Akita University.

Rakotondravaly, D. A., & Randrianja, R. (2022). Petrology and Geochemistry of the Granitic Rocks from the Itremo Domain, Central Madagascar. *Journal of Geosciences and Geomatics, 10,* 31-44. https://doi.org/10.12691/jgg-10-1-3

Rasoamalala, V., Salvi, S., Béziat, D., Ursule, J., Cuney, M., Parseval (De), P. et al. (2014). Geology of Bastnaesite and Monazite Deposits in the Ambatofinandrahana Area, Central Part of Madagascar: An Overview. *Journal of African Earth Sciences, 94,* 128-140. https://doi.org/10.1016/j.jafrearsci.2013.11.009

Ravoniarisoa, C., & Rakotomanana, D. (2002). *Contribution à la Connaissance de la*

Gîtologie de la Bastnaësite d'Ankaditany Marovoalavo (Région d'Ambatofinandrahana). Unpublished Thesis, Antananarivo, Madagascar: Econle Supérieure Polytechnique d'Antananarivo, Université d'Antananarivo. http://biblio.univ-antananarivo.mg/pdfs/ravoniarisoaclarisse_espa_ing_02.pdf

Roig, J. Y., Tucker, R. D., Peters, S. G., Delor, C., & Theveniaut, H. (2012). *Carte Géologique de la République de Madagascar à 1/1 000 000.* Ministère des Mines, Direction de la Géologie, Projet de Gouvernance des Ressources Minérales.

Schmidt, M. W. (1992). Amphibole Composition in Tonalite as Function of Pressure: An Experimental Calibration of Al-in-Hornblende Barometer. *Contributions to Mineralogy and Petrology, 110,* 304-310. https://doi.org/10.1007/BF00310745

Spencer, K. J., & Lindsley, D. H. (1981). A Solution MODEL for coexisting iron-Titanium Oxides. *American Mineralogist, 66,* 1189-1201.

Taylor, A. W. (1964). Phase Equilibria in the System FeO-Fe_2O_3-TiO_2 at 1300˚C. *American Mineralogists, 49,* 1016-1030.

Tischendorf, G., Gottesmann, B., Förster, H.-J., & Trumbull, R. B. (1997). On Li-Bearing Micas: Estimating Li from Electron Microprobe Analyses and an Improved Diagram for Graphical Representation. *Mineralogical Magazine, 61,* 809-834. https://doi.org/10.1180/minmag.1997.061.409.05

Tucker, R. D., Ashwal, L. D., Handke, M. J., Hamilton, M. A., Le Grange, M., & Rambeloson, R. A. (1999). U–Pb Geochronology and Isotope Geochemistry of the Archean and Proterozoic Rocks of North-Central Madagascar. *The Journal of Geology, 107,* 135-153. https://doi.org/10.1086/314337

Tucker, R. D., Kusky, T. M., Buchwaldt, R., & Handke, M. J. (2007). Neoproterozoic Nappes and Superposed Folding of the Itremo Group, West-Central Madagascar. *Gondwana Research, 12,* 356-379. https://doi.org/10.1016/j.gr.2006.12.001

Tucker, R. D., Peters, S. G., Roig, J. Y., Théveniaut, H., & Delor, C. (2012). *Notice Explicative des Cartes Géologiques et Métallogéniques de la République de Madagascar à 1/1 000 000.* Ministère des Mines.

Tucker, R. D., Roig, J. Y., Moine, B., Delor, C., & Peters, S. G. (2014). A Geological Synthesis of the Precambrian Shield in Madagascar. *Journal of African Earth Sciences, 94,* 9-30. https://doi.org/10.1016/j.jafrearsci.2014.02.001

Yang, X.-A., Chen, Y.-C., Liu, S.-B., Hou, K.-J., Chen, Z.-Y., & Liu, J.-J. (2015). U–Pb Zircon Geochronology and Geochemistry of Neoproterozoic Granitoids of the Maevatanana Area, Madagascar: Implications for Neoproterozoic Crustal Extension of the Imorona–Itsindro Suite and Subsequent Lithospheric Subduction. *International geology Reviews, 57,* 1633-1649. https://doi.org/10.1080/00206814.2014.977969

Yoshida, M. (1998). Proterozoic Geology of Madagascar: International Field Workshop of IGCO-348/368 in 1997. *Gondwana Research, 1,* 299-301. https://doi.org/10.1016/S1342-937X(05)70841-8